

I. MEASURING THE TOPOLOGY OF LARGE-SCALE STRUCTURE IN THE UNIVERSE*

J. RICHARD GOTT III

Department of Astrophysical Sciences, Princeton University, Princeton, New Jersey 08544

ABSTRACT

An algorithm for quantitatively measuring the topology of large-scale structure developed by our group has now been applied to a large number of observational data sets (Gott *et al.* 1988). The present paper summarizes and provides an overview of some of these observational results. On scales significantly larger than the correlation length, $\lambda \gtrsim 1200 \text{ km s}^{-1}$, the cluster and galaxy data are fully consistent with a sponge-like random phase topology. At a smoothing length of $\lambda \sim 600 \text{ km s}^{-1}$, however, the observed genus curves show a small shift in the direction of a meatball topology. Cold dark matter (CDM) models show similar shifts at these scales but not generally as large as those seen in the data. Bubble models, with voids completely surrounded on all sides by walls of galaxies, show shifts in the opposite direction. The CDM model is overall the most successful in explaining the data.

Key words: cosmology—structure of the universe—universe models

I. Introduction

Recent deep redshift surveys by de Lapparent, Geller, and Huchra (1986), Kirshner *et al.* (1981), Haynes and Giovanelli (1986), and Tully and Fisher (1987) have renewed interest in the topology of large-scale structure in the universe. The distribution of galaxies on large scales has been variously described as a hierarchy of clusters (Soneira and Peebles 1987; Bhavsar 1978, 1980), an irregular lattice of cells or “bubbles” (Joeveer and Einasto 1978; de Lapparent *et al.* 1986), or a network of filaments (Einasto *et al.* 1984; Haynes and Giovanelli 1986; Bhavsar and Ling 1988). One might describe the topology of these models as, respectively, a “meatball” topology, a “Swiss-cheese” topology, and a “sponge” topology (Gott, Melott, and Dickinson 1986, hereafter GMD).

In a recent series of papers we have developed techniques for quantitatively measuring the topology of large-scale structure, extending the approach of GMD. (See Gott, Weinberg, and Melott (1987, hereafter GWM) for a brief introduction to the method; for further results and more detailed discussions see Hamilton, Gott, and Weinberg (1986), Weinberg, Gott, and Melott (1987), Melott, Weinberg, and Gott (1988), and Gott, Jeffrey, Weinberg, and Melott (1989), hereafter HGW, WGM, MWG, and GJWM, respectively.) We have now applied these techniques to a large number of observational data sets (Gott *et al.* 1988). The present paper summarizes and provides an overview of some of these observational results.

II. Method

A. The Genus Curve

When analyzing the topology of a distribution of galaxies we are presented with a series of points (galaxies) distributed in a nonuniform fashion in three-dimensional space. We are interested in the structures formed by the galaxies and not in the fact that they are isolated points. So the first thing we do is to smooth the data with a Gaussian smoothing function, $W \propto \exp(-r^2/\lambda^2)$, where r is the distance and λ is a smoothing length picked to be larger than the mean galaxy-galaxy separation $\bar{d} = n^{-1/3}$ (where n is the number density of galaxies in the sample). Information on the topology is then carried in the density contour surfaces of this smoothed density distribution. If we want to study the nature of the topology on different scales we can adopt different smoothing lengths.

We define the genus of the contour surface as

$$G_s = (\text{No. of holes}) - (\text{No. of isolated regions}), \quad (1)$$

where “hole” means a hole like a doughnut has and where an isolated (i.e., compact) region may be above or below the threshold density (GMD, GWM). A sponge has a positive genus since its surface is all in one piece and it is multiply connected with many holes. Using the Gauss-Bonnet theorem, GMD show that G_s is equal to $-(4\pi)^{-1}$ times the integral of the Gaussian curvature K over the contour surface. This makes it possible to write a computer program which will measure the genus of a contour surface. In a pixelated array the contour surface is a corrugated one which follows the pixels and the Gaussian curvature is concentrated in delta functions at the vertices. The computer program calculates $\int K dA$ by simply

*Paper based on lecture given at the workshop on the Topology of the Large-Scale Structure of the Universe held at Lawrence, Kansas, 1988 April 26–29.

adding the contributions from each vertex. The computer program is described in detail in GMD. Copies of this program may be obtained by interested users from David Weinberg at Princeton, and a listing of the program will be published in Weinberg (1988, in this volume) and in Melott (1989).

One can derive a formula for the genus-per-unit volume in Gaussian initial conditions. In the standard big-bang inflationary model the small amplitude fluctuations present at recombination (and out of which the structures we see today grow by gravitational instability) arise from random quantum fluctuations that are Gaussian with random phases (Bardeen *et al.* 1986; Bardeen, Steinhardt, and Turner 1983). As long as the fluctuations stay in the linear regime they all grow at the same rate, and any damping affects positive and negative fluctuations equally. Thus, after recombination we have to a good approximation random-phase Gaussian fluctuations, with a power spectrum $P(k)$ which can be calculated for the cold dark matter (CDM) (Peebles 1982; Blumenthal *et al.* 1984) or heavy neutrino (Zeldovich, Einasto, and Shandarin 1982) models directly from the primordial Zeldovich inflationary spectrum. We can now apply our topology-measuring algorithm to such a set of initial conditions. We smooth the data with a smoothing length λ , giving a smoothed power spectrum

$$P'(k) = P(k)e^{-k^2\lambda^2/2},$$

and construct density contours. Let ν be the number of standard deviations by which the contour threshold density δ_c is above or below the average density, so that the volume fraction on the high-density side of the contour is

$$f = (2\pi)^{-1/2} \int_{\nu}^{\infty} e^{-t^2/2} dt. \quad (2)$$

Then HGW (and also Bardeen *et al.* (1986), Doroshkevich (1970), Adler (1981) who used the formula to count high-density peaks) showed that the mean genus-per-unit volume is given by

$$g_s = N(1-\nu^2)e^{-\nu^2/2}, \quad (3)$$

where

$$N = \frac{1}{(2\pi)^2} \left(\frac{\int k^2 P'(k) d^3k}{3 \int P'(k) d^3k} \right)^{3/2}. \quad (4)$$

Notice that while the amplitude of the genus curve depends on N and therefore on $P(k)$, the shape of the genus curve as a function of density enhancement, $g_s \propto (1-\nu^2)e^{-\nu^2/2}$, is independent of the power spectrum. Since N is positive definite the median density contour, $f = 0.5$, $\nu = 0$, is always spongelike with $g_s > 0$ regardless of the initial power spectrum. For $f < 0.16$, $\nu > 1.0$, g_s is negative and we see isolated clusters, and for $f > 0.84$, ν

< -1.0 , g_s is again negative and we see isolated voids.

As long as fluctuations remain in the linear regime they grow in place, simply increasing in amplitude, and the density contour surfaces as a function of ν do not change. When we smooth on a scale $\lambda \gtrsim r_0$ where r_0 is the correlation length (the place where the covariance function amplitude drops to unity, $\xi(r_0) = 1$), we are looking at scales that are only just beginning to come out of the linear regime, and the density contours and genus curves should reflect those of the initial conditions. Our studies of numerical simulations show that this is indeed the case for hierarchical clustering models like CDM. Likewise, standard biasing techniques do not change the results appreciably because they make the mass-to-light ratio a monotonic function of a total density, so that contours of constant mass density are also contours of constant luminosity density. Provided we identify contours by volume fraction f , contours in the biased "galaxy" distribution are very close to those in the unbiased mass distribution (GWM).

B. Numerical Simulations

In Section IV we compare the observations to numerical simulations of cold dark matter and massive neutrino scenarios. These are particle-mesh (PM) simulations which accurately follow the gravitational evolution of the collisionless dark matter. The simulation methods are discussed extensively in MWG, to which we refer the reader for details. We also analyze "toy-model" bubble distributions, constructed as in GWM and WGM. We place bubble centers randomly with a mean separation D , then place galaxies only in pixels that are equidistant from the two nearest centers. This creates a distribution of irregular, polyhedral bubbles with mean volume D^3 each and typical diameters of order D .

We have analyzed discretely-sampled versions of our numerical models and arrived at a number of useful rules of thumb (GJWM; see also GWM, WGM, and MWG). First, one should use a smoothing length $\lambda \geq 2.5$ pixels so that the random-phase formula is accurately followed and no finite pixel-size corrections (HGW) need be applied. Second, one should use $\lambda \geq \bar{d}$ (the mean galaxy-galaxy separation); otherwise discreteness produces an unwanted shift in the "meatball" direction because we pick up single galaxies in low-density regions. In models where the covariance function is approximated by $\xi(r) \sim (\delta\rho/\rho)^2 \sim (r/r_0)^{-2}$ the true density fluctuations will be masked by Poisson sampling noise unless

$$\frac{\lambda}{\bar{d}} \geq \frac{1\bar{d}^2}{\pi^{3/2}r_0^2}. \quad (5)$$

All our observational samples are smoothed with $\lambda \geq 2.5$ pixels and $\lambda \geq \bar{d}$ and satisfy equation (5).

With a smoothing length of $\lambda \geq \bar{d}$ that satisfies equation (5), one correctly recovers the topology of the underlying

density field for distributions that are only mildly nonlinear. However, clustering accentuates discreteness effects, and for very nonlinear distributions $\lambda \geq \bar{d}$ may not be sufficient to suppress the artificial “meatballing” that can occur when a density field is sparsely sampled.

Experiments with bubble distributions show that one can easily detect the characteristic asymmetry in the genus curve (a peak at $\nu > 0$) provided $\bar{d} \leq \lambda \leq D/4$, where D is the typical bubble diameter. Heavens (1985) shows that a cubical array of bubbles of diameter D produces a covariance function with $r_0 = D/8$, so the observed r_0 of 500 km s^{-1} could be produced by bubbles with $D \sim 4000 \text{ km s}^{-1}$. De Lapparent *et al.* (1986) suggest that the structure in their “slice of the universe” survey is produced by bubbles with typical diameters of $2500 \text{ km s}^{-1} < D < 5000 \text{ km s}^{-1}$, quite in line with what one might expect from the covariance function. Since $D \sim 8 r_0$, we should easily detect bubbles in a study with $\lambda = \bar{d} = r_0$.

C. Techniques for Observational Samples

Observational samples typically involve oddly-shaped conical regions with the Earth at the apex. A typical survey covers a certain region of the sky of Ω_s steradians out to a fixed redshift distance $r_{\text{max}} = H_0^{-1} V_{\text{max}}$. First let us consider the simple case of a volume-limited survey. We adopt a smoothing length λ greater than or equal to the mean galaxy-galaxy separation and pick a pixel size, small enough that $\lambda \geq 2.5$ pixel.

We display the data in a cubical pixelated array, typically $64 \times 64 \times 64$, which is large enough to comfortably include the observational region. In calculating the genus curve we only integrate KdA over the “active” vertices whose surrounding eight pixels are all within the survey volume.

Since we are smoothing we need to know what to assume about the pixels beyond the survey region. The simplest choice is just to assume that they are at the average density. The fact that some contour surfaces will cross the boundary is perfectly all right because the topology routine correctly measures just the part that it sees. However, the density of pixels that lie within one smoothing length of the boundary will be affected by our assumption of a uniform, average density exterior.

We would like some estimate of the uncertainty in our measurement of topology, a way to put error bars on our genus curves. As an extreme example we may have two clusters joined by a filament which depends crucially on one galaxy in the middle to form (i.e., if we removed that one galaxy from the survey the filament would break lowering the genus by 1). Such a case (if we view the galaxies as chosen by some sampling process from an underlying distribution) should introduce an uncertainty in the genus of order ± 1 . On the other hand, a filament formed by several galaxies would be on much more solid ground.

We estimate the statistical errors in the genus using the statistical bootstrap method pioneered by Barrow, Bhavsar, and Sonoda (1984), who used it to estimate the errors in the covariance function. This method is powerful and very easy to apply. Suppose, for example, we have 877 galaxies in a volume-limited survey. We have 877 positions for these galaxies. We take the 877 galaxies out and throw them randomly back at those 877 positions. After such a replacement run has been made some of the positions will have no galaxies in them and some will have one, two, or more galaxies in them with the probabilities given by the Poisson formula $P(N) = (N!)^{-1} e^{-1}$. The replacement run (except at zero separation) will have on average the same 2, 3, and higher point correlation functions as the original sample, with appropriate fluctuations about the mean.

To return to our example, there will be a 37% chance ($P(0) = e^{-1}$) that the galaxy location crucial for forming the filament will not be filled and the genus will be lowered by 1. This is an extreme example where the presence or absence of just one galaxy changes the large-scale structure. One would expect this not to be the case most of the time. If we do a number of replacement runs and calculate the genus curve for each we will get a good estimate of the statistical uncertainty in the genus curve. Features that are formed by many galaxies will virtually always show up on the replacement run.

For volume-limited surveys we first analyze the distribution itself with a uniform, average density exterior for smoothing. We then generate 12 bootstrap resamplings of the data and smooth each of these with an exterior that is a Poisson distribution of particles with the correct mean density. The error bars show the run-to-run dispersion of the bootstrap results. As expected, in most plots the raw galaxy data fall within the bootstrap error bars about 2/3 of the time. The average over 12 resamplings smooths out the “noise” in the genus curve, and the sizes of the error bars show what features of the curve are to be trusted.

From tests on numerical simulations we find that the statistical bootstrap technique works extremely well as a way of estimating uncertainties in the genus curve. The bootstrap error bars are very similar to those found by (a) taking different Poisson samplings of the same underlying density field or (b) measuring the run-to-run dispersion from different simulations. If anything, the 1- σ bootstrap errors are somewhat conservative. The only penalty we pay for using the bootstrap technique is that, since a fraction $P(0) = e^{-1}$ of the locations will not harbor a galaxy in the replacement run, the effective mean separation of independent points grows by a factor of $(1 - e^{-1})^{-1/3} = 1.17$. The increase in discreteness tends to produce a slight meatball asymmetry when $\lambda = \bar{d}$, a systematic effect that disappears when $\lambda = 1.2 \bar{d}$.

Now what do we do with samples that are either size or magnitude limited rather than volume limited? First we

compute the selection function $\rho_s(r)$. The selection function gives the run of density with radius we would expect to see in the sample if the galaxies were distributed uniformly. We can calculate the selection function provided we know for each galaxy the maximum distance $D_{\max,i}$ out to which it could have been detected by the survey. The maximum number of "resolution elements" is achieved by setting the outer boundary such that the function $F(r) = \rho_s(r) r^3$ reaches its maximum value at $r = r_{\max}$. We do the statistical bootstrap replacement just as in the volume-limited samples, but for the exterior region we now do a Poisson placement of points with number density $\bar{n}(r) = \rho_s(r)$ for $r \leq r_{\max}$ and $\bar{n}(r) = \rho_s(r_{\max})$ for $r > r_{\max}$. Before doing the smoothing we divide the counts in each pixel by the expected number, in a smooth unclustered distribution. We smooth with a smoothing length λ equal to the expected mean interparticle separation at the outer edge of the sample.

III. Observations

On the largest scales we study the topology using a virtually complete, volume-limited sample of Abell clusters with $z < 0.08$, $\delta > -27^\circ$, $|b| > 40^\circ$, with redshifts taken from Struble and Rood (1987), Hoessel, Gunn, and Thuan (1980), and Thuan (1980). We convert redshifts to velocities with the formula $V_i = 2c[1 - (1 + z_i)^{-1/2}]$ which plots the clusters at their correct comoving distances in an $\Omega = 1$ matter-dominated cosmology. (For our galaxy samples (all have $V_{\max} \leq 11,800 \text{ km s}^{-1}$) the low-velocity formula $V_i = cz_i$ is quite adequate and has been adopted.) In all our samples, galaxies (or clusters) are plotted at their redshift distances and distances are measured in km s^{-1} . Our smoothing length for the Abell sample, $\lambda = 5000 \text{ km s}^{-1}$, is slightly larger than the mean interparticle separation and satisfies equation (5). Our pixel size is 1000 km s^{-1} . Bahcall and Soneira (1983) find that the clusters in this sample have a correlation length of $r_0 \sim 2500 \text{ km s}^{-1}$. The covariance amplitude of Abell clusters greatly exceeds that of galaxies, presumably because of biasing effects (Kaiser 1984; cf. also Hamilton and Gott 1988). The clustering of Abell clusters produces fluctuations large enough to give us a detectable signal with $\lambda = 5000 \text{ km s}^{-1}$ (cf. eq. (5)), and it allows us to examine scales where the fluctuations in the total mass density are clearly still in the linear regime.

The genus curve for this sample appears in Figure 1. Open squares show the results for the cluster data smoothed with the average density exterior. Filled circles show the average of 12 bootstrap resamplings, each smoothed with a Poisson realization of the exterior. Error bars are the run-to-run dispersion of the bootstrap resamplings. The topology is an excellent fit to the random-phase model (cf. eq. (3)), which is shown as a solid line for comparison. The amplitude of the theoretical random-phase genus curve is set by minimizing the value of χ^2 for

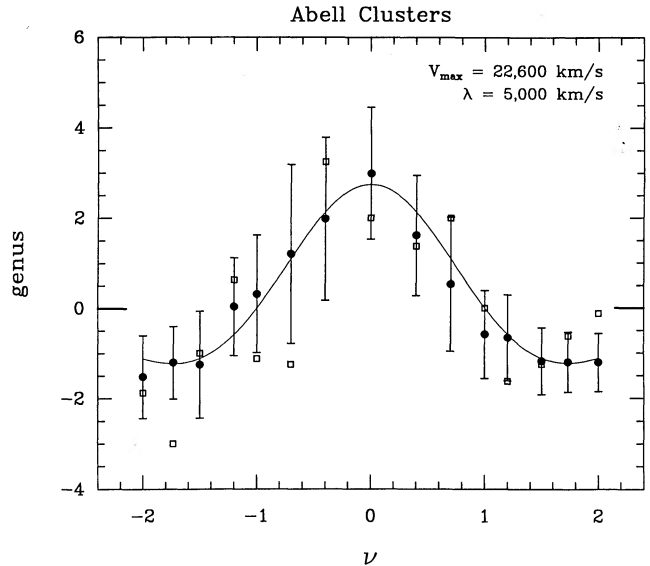


FIG. 1—The genus curve for the Abell cluster sample ($V_{\max} = 22,600 \text{ km s}^{-1}$, $\lambda = 5000 \text{ km s}^{-1}$) plotted with the best-fit random-phase theoretical curve $g_s \propto (1 - \nu^2) e^{-\nu^2/2}$. The mean values shown as filled circles and the error bars are computed from the statistical bootstrap technique. The unfilled squares are obtained from simply taking the raw data and assuming exactly average density in the universe beyond the observational sample. The overall genus curve is well fit by the random-phase theoretical curve.

the fit to the bootstrap data points treating them as if they were independent.

Two volume-limited subsets have been prepared from the Haynes and Giovanelli (1986) sample of over 4000 redshifts. These samples extending to $V_{\max} = 11,800 \text{ km s}^{-1}$ and $V_{\max} = 6500 \text{ km s}^{-1}$, respectively, cover roughly the region with $\delta > 0$, $b < -30^\circ$, and $22 \text{ h} < \alpha < 4 \text{ h}$.

The Giovanelli and Haynes volume-limited sample with $V_{\max} = 11,800 \text{ km s}^{-1}$ contains 419 galaxies and has a pixel size of 400 km s^{-1} . When this sample is smoothed at $\lambda = 1200 \text{ km s}^{-1}$ its topology is also a good fit to the theoretical random-phase curve, showing isolated voids at low density, a sponge-like topology at the median-density contour, and isolated clusters at high density. This result combined with the Abell data in Figure 1 indicates that with λ significantly larger than r_0 we obtain the random-phase spongelike topology expected from the standard model in which the structure we see today originated from random quantum noise in the early universe.

Our CfA sample is drawn from the Huchra *et al.* (1983) survey, which has a magnitude limit of $m_b = 14.5$. The survey is divided into north ($b > 40^\circ$ and $\delta > 0^\circ$) and south ($b < -30^\circ$ and $\delta > -2:5$) galactic caps. To optimize our resolution we chose a sample with $V_{\max} = 5000 \text{ km s}^{-1}$ (pixel size 150 km s^{-1}) which we smoothed at $\lambda = 650 \text{ km s}^{-1}$. While the median contour is spongelike, its genus curve (Fig. 2) shows a small shift to the left toward a meatball topology.

A similar but even larger meatball shift shows up in the

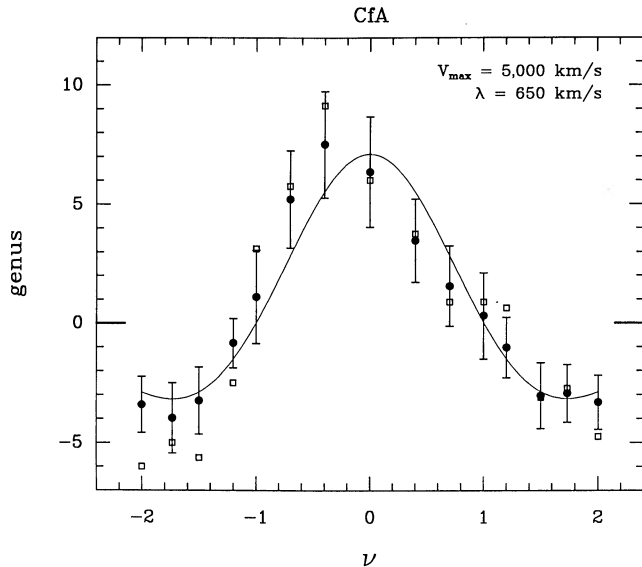


FIG. 2—The genus curve for the CfA, $V_{\max} = 5000 \text{ km s}^{-1}$ sample which shows a small shift to the left in the direction of a meatball topology. Symbols as in Figure 1.

GH volume-limited sample with $V_{\max} = 6500 \text{ km s}^{-1}$, having 877 galaxies, a pixel size of 200 km s^{-1} , and smoothed with $\lambda = 600 \text{ km s}^{-1}$. This shift reflects the fact that the Perseus-Pisces supercluster dominates the sample. The hallmark of a “meatball” topology is that the “isolated clusters” are more prominent than in a random-phase distribution, so the existence of the Perseus-Pisces supercluster as such a prominent entity in the sample produces the “meatball” shift in the curve.

As outlined in HGW, while the shape of the random-phase genus curve is independent of scale and of the power spectrum, the amplitude of the genus curve does depend on the power spectrum and on the smoothing scale λ (eq. (4)). By plotting the amplitude $g_s(0)$ of the best-fitting random-phase genus-per-unit-volume curve as a function of λ for our different observational samples we can learn something about the shape of the power spectrum. For this study we used all of the data samples we have analyzed including the Thuan and Schneider (1988) dwarf sample (TS) ($\delta > 0$, $|b| > 40^\circ$, out to $V_{\max} = 3000 \text{ km s}^{-1}$) and the Tully (1987) sample ($|b| > 40^\circ$, out to $V_{\max} = 3000 \text{ km s}^{-1}$) (cf. Tully and Fisher 1987). The results show that as we use smaller and smaller values of λ we discover a higher and higher volume density of holes. We discover ever-choppier substructure as we look at smaller and smaller scales. This type of behavior is expected when there is no cutoff in the power spectrum at small scales. We have calculated $g_s(0)$ as a function of λ using the CDM power spectrum of Davis *et al.* (1985) with the standard value of $\Omega h = 0.5$ and equations (3) and (4) with no free fitting parameters at all. This curve is independent of the amplitude of the fluctuations and the

amount of biasing but does not include possible nonlinear evolution or discrete sampling effects. The fit of the CDM curve to the data is remarkably good.

IV. Discussion

On scales significantly larger than the correlation length, $\lambda \geq 1200 \text{ km s}^{-1}$, the cluster and galaxy data are fully consistent with a random-phase topology. At a smoothing length of $\lambda \sim 600 \text{ km s}^{-1}$, however, the observed genus curves show a small shift in the direction of a meatball topology.

To further study these results we have prepared an extensive series of numerical simulations from which we can create “simulated data” to compare directly with the observations. These simulated data sets have the same distance selection effects as the observations and are analyzed in exactly the same fashion as the observations. Our procedure ignores the effects of peculiar velocities, but we have shown elsewhere (MWG) that including peculiar velocities causes no appreciable difference in the topology when the smoothing length is $\geq 600 \text{ km s}^{-1}$.

While the CDM model on scales of $\lambda \sim 600 \text{ km s}^{-1}$ has an underlying mass distribution which is random phase (GWM), biasing combined with sparse sampling can provide meatball shifts. Five CDM simulations of the CfA data set with $\lambda = 650 \text{ km s}^{-1}$ were done. Four showed slight shifts in the meatball direction while one showed a shift that was just as large as that seen in the real CfA sample. We did four CDM simulations of the GH $V_{\max} = 6500 \text{ km s}^{-1}$ sample with $\lambda = 600 \text{ km s}^{-1}$. One of the four simulations showed a meatball shift very nearly as large as that seen in the GH sample. The other three looked basically random phase. This confirms the picture that the CDM model is able to produce meatball shifts like those seen in the observational data but that the effect is just not as strong. The individual neutrino simulations produced a variety of genus-curve shapes none of which looked quite like the observed data. (This is not surprising since because of the large coherence length in the neutrino model a survey region may include only a small number of structures, making individual simulations look erratic.) We ran bubble simulations with bubble diameters of 2500 km s^{-1} , 3200 km s^{-1} , and 4000 km s^{-1} . Out of 12 bubble simulations of the GH, $\lambda = 600 \text{ km s}^{-1}$ data set (four for each bubble diameter), all 12 showed a shift to the right in the bubble direction. Out of 12 bubble simulations of the small CfA $\lambda = 650 \text{ km s}^{-1}$ data set (four for each bubble diameter), eight showed a shift in the bubble direction and four were roughly random phase. Thus, if bubbles with diameters in the range 2500 km s^{-1} to 4000 km s^{-1} were present in the samples they would have had ample opportunity to have shown their presence. In fact, shifts in the opposite direction were seen. Thus, we find no evidence for bubbles with sizes in the range 2500 km s^{-1} to 4000 km s^{-1} . In saying that we find no evidence for

bubbles in the data we should emphasize that we do not mean to say the data have no voids. Of course these observational data sets contain a number of voids and quite empty ones at that. It is just that the voids are not surrounded on all sides by walls of galaxies (that is the bubble topology); rather, the voids are connected to other voids by low-density tunnels (as occurs in a sponge-like topology).

The failure to find bubbles should perhaps come as no great surprise. While the first de Lapparent *et al.* (1986) slice does bear a striking resemblance to "suds in the kitchen sink", subsequent slices from the extended CfA survey (Huchra 1988) present a somewhat more-muddled appearance. Slices from the Giovanelli and Haynes survey show a heterogeneous mix of structures, including the Perseus-Pisces supercluster which is clearly a filament rather than a sheet. Studies of individual voids show that they are not completely surrounded by galaxy walls but flow into neighboring low-density regions (Burns, private communication; Gregory, private communication; Kirshner *et al.* 1987). Slices from biased CDM simulations by White *et al.* (1987) reproduce the visual impression of the CfA slices extremely well, but CDM models have a sponge-like rather than bubble-like topology. As we have pointed out elsewhere, a slice through a sponge can look very much like a slice through bubbles, although one can, in principle, distinguish the two topologies by quantitative analysis even of two-dimensional surveys (Melott *et al.* 1988). Our results suggest that biased CDM models like those of White *et al.* (1987) offer a more-promising explanation than simple bubble models for the "frothy" appearance of large-scale structure.

Of the models that we have examined in detail, CDM comes the closest to explaining the observed topology. While the combination of biasing and discreteness can lead to a slight meatball shift, the CDM model in its current form does not produce as strong a meatball effect as seen in our observational data sets at $\lambda \sim 600 \text{ km s}^{-1}$. We are tempted to wonder what sorts of effects could enhance the meatball shifts already seen in the CDM models and bring them into even better agreement with the observational data. The fluctuation amplitude and degree of biasing in the standard CDM model produce a galaxy correlation length of $\sim 500 \text{ km s}^{-1}$. If the galaxy correlation length is not 500 km s^{-1} as usually assumed, but is really as high as $\sim 750 \text{ km s}^{-1}$ as suggested by de Lapparent, Geller, and Huchra (1988), a stronger biasing procedure or more nonlinear dynamical evolution will be needed to bring the CDM model in line with the galaxy covariance function. The same modifications might also improve the agreement with our topology results, since nonlinear clustering and extreme biasing both tend to increase the prominence of clusters and move a random-phase topology toward a meatball topology.

The future prospects for these techniques are bright.

Data from the southern-sky redshift survey (da Costa *et al.* 1988) and the IRAS redshift survey (Strauss and Davis 1988) should become available in the next year or two. In a few more years data from the extended CfA survey and, perhaps, from surveys by dedicated redshift telescopes will allow us to measure topology on a variety of scales with good statistical accuracy.

Funds for preparing this review and for attending the Lawrence, Kansas Topology Workshop have been provided by NSF grant AST 87-21484 and by NASA Astrophysical Theory grant NAGW-765.

REFERENCES

- Adler, R. J. 1981, *The Geometry of Random Fields* (Chichester: Wiley).
- Bahcall, N. A., and Soneira, R. M. 1983, *Ap. J.*, **270**, 20.
- Bardeen, J. M., Bond, J. R., Kaiser, N., and Szalay, A. S. 1986, *Ap. J.*, **304**, 15.
- Bardeen, J. M., Steinhardt, P., and Turner, M. 1983, *Phys. Rev. D*, **28**, 679.
- Barrow, J. D., Bhavsar, S. P., and Sonoda, D. M. 1984, *M.N.R.A.S.*, **210**, 19p.
- Bhavsar, S. P. 1978, *Ap. J.*, **222**, 412.
- . 1980, *Ap. J.*, **237**, 671.
- Bhavsar, S. P., and Ling, E. N. 1988, *Ap. J. (Letters)*, **331**, L63.
- Blumenthal, G. Faber, S. M., Primack, J. R., and Rees, M. J. 1984, *Nature*, **311**, 517.
- Davis, M., Efstathiou, G., Frenk, C. S., and White, S. D. M. 1985, *Ap. J.*, **292**, 371.
- de Costa, L. N., *et al.* 1988, *Ap. J.*, **327**, 544.
- de Lapparent, V., Geller, M. J., and Huchra, J. P. 1986, *Ap. J. (Letters)*, **302**, L1.
- . 1988, CfA Preprint 2636.
- Doroshkevich, A. G. 1970, *Astrofizika*, **6**, 581 (English transl. in *Astrophysics*, **6**, 320 (1970)).
- Einasto, J., Klypin, A. A., Saar, E., and Shandarin, S. F. 1984, *Ap. J.*, **206**, 529.
- Gott, J. R., Jeffrey, S., Weinberg, D. Y., and Melott, A. L. 1989, in preparation (GJWM).
- Gott, J. R., Melott, A. L., and Dickinson, M. 1986, *Ap. J.*, **306**, 341 (GMD).
- Gott, J. R., Miller, J., Thuan, T. X., Schneider, S. E., Weinberg, D., Gammie, C., Polk, K., Vogeley, M., Jeffrey, S., Bhavsar, S. P., Melott, A. L., Giovanelli, R., Haynes, M. P., Tully, R. B., and Hamilton, A. J. S. 1988, *Ap. J.*, submitted.
- Gott, J. R., Weinberg, D. H., and Melott, A. L. 1987, *Ap. J.*, **319**, 1 (GWM).
- Hamilton, A. J. S., and Gott, J. R. 1988, *Ap. J.*, **331**, 641.
- Hamilton, A. J. S., Gott, J. R., and Weinberg, D. H. 1986, *Ap. J.*, **309**, 1 (HGW).
- Haynes, M. P., and Giovanelli, R. 1986, *Ap. J.*, **306**, L55.
- Heavens, A. 1985, *M.N.R.A.S.*, **213**, 143.
- Hoessel, J. C., Gunn, J. E., and Thuan, T. X. 1980, *Ap. J.*, **241**, 486.
- Huchra, J. 1988, in *IAU Symposium on Large Scale Structure, Hungary*, ed. J. Adouze and A. Szalay (Dordrecht: Reidel), in press.
- Huchra, J., Davis, M., Latham, D., and Tonry, J. 1983, *Ap. J. Suppl.*, **52**, 89.
- Joeveer, M., and Einasto, J. 1978, in *IAU Symposium 79, The Large Scale Structure of the Universe*, ed. M. S. Longair and J. Einasto (Dordrecht: Reidel), p. 241.
- Kaiser, N. 1984, *Ap. J. (Letters)*, **276**, L9.
- Kirschner, R. P., Oemler, A., Schechter, P. L., and Schectman, S. A. 1981, *Ap. J. (Letters)*, **248**, L57.
- . 1987, *Ap. J.*, **314**, 493.
- Melott, A. L. 1989, *Phys. Rep.*, in preparation.

- Melott, A. L., Cohen, A. P., Hamilton, A. J. S., Gott, J. R., and Weinberg, D. H. 1988, in preparation.
- Melott, A. L., Weinberg, D. H., and Gott, J. R. 1988, *Ap. J.*, **328**, 50 (MWG).
- Peebles, P. J. E. 1982, *Ap. J. (Letters)*, **263**, L1.
- Soneira, R. M., and Peebles, P. J. E. 1987, *Ap. J.*, **83**, 845.
- Strauss, M. A., and Davis, M. 1988, in *IAU Symposium 130*, ed. J. Audouze and A. Szalay (Dordrecht: Reidel), in press.
- Struble, M. F., and Rood, H. J. 1987, *Ap. J. Suppl.*, **63**, 543.
- Thuan, T. X. 1980, in *Physical Cosmology*, ed. R. Balian, J. Audouze, and D. N. Schramm (New York: North Holland), p. 278.
- Thuan, T. X., and Schneider, S. 1988, in preparation.
- Tully, R. B. 1987, *Ap. J.*, **323**, 1.
- Tully, R. B., and Fisher, J. R. 1987, *Nearby Galaxies Atlas* (Cambridge: Cambridge University Press).
- Weinberg, D. H. 1988, *Pub. A.S.P.*, 1988, **100**, 1373.
- Weinberg, D. H., Gott, J. R., and Melott, A. L. 1987, *Ap. J.*, **321**, 2 (WGM).
- White, S. D. M., Frenk, C., Davis, M., and Efstathiou, G. 1987, *Ap. J.*, **313**, 505.
- Zeldovich, Ya. B., Einasto, J., and Shandarin, S. F. 1982, *Nature*, **300**, 407.